Biomass Conversion and Biorefinery (2024) 14:8283–8292
https://doi.org/10.1007/s13399-022-03079-8

ORIGINAL ARTICLE

Dynamic simulation of lead(II) metal adsorption from water on activated carbons in a packed-bed column

Areeba Hameed[1] · Bassim H. Hameed[1] · Fares A. Almomani[1] · Muhammad Usman[2] · Muneer M. Ba-Abbad[3] · Majeda Khraisheh[1]

Received: 22 March 2022 / Revised: 23 June 2022 / Accepted: 11 July 2022 / Published online: 29 July 2022
© The Author(s) 2022

Abstract
In this work, lead(II) adsorption on activated carbons, tire-derived activated carbon (TAC), and commercial activated carbon (CAC), in a packed-bed column, was simulated using the Aspen Adsorption® V11 flowsheet simulator. The simulator was used to model the fixed-bed adsorption column and to establish the breakthrough curves by varying the initial concentration of lead(II) ions (500 mg/L, 1000 mg/L, 2000 mg/L, and 3000 mg/L), the bed height (0.2 m, 0.3 m, 0.4 m, 0.5 m, and 0.6 m), and the flow rate (9.88×10^{-4} m^3/s, 1.98×10^{-3} m^3/s, 2.96×10^{-3} m^3/s, 3.95×10^{-3} m^3/s, and 4.94×10^{-3} m^3/s), at constant temperature and pressure of 25 °C and 3 bar, respectively. At the optimum conditions of 500 mg/L lead(II) concentration, 0.6 m bed height, and 9.88×10^{-4} m^3/s flow rate, the breakthrough times were 488 s and 23 s for TAC and CAC, respectively. Under the same conditions, the adsorption capacity obtained at $t_{0.5}$ was 114.26 mg/g for TAC and 7.72 mg/g for CAC. The simulation results indicate the potential of TAC for the adsorption of lead(II) in comparison to CAC.

Keywords Activated carbon · Adsorption · Lead(II) · Breakthrough curve · Aspen adsorption simulator

1 Introduction

During oil and gas operations, large volumes of wastewater are produced, which is referred to as produced water (PW). This water is by far the most generated by industry and includes a variety of pollutants such as oil compounds, dissolved minerals, chemical compounds, and dissolved particles [1]. Zinc, lead, manganese, iron, and barium are among the frequent metals detected in PW [2]. The removal and recovery of toxic heavy metals have received a lot of attention in recent years. Discarding PW without sufficient treatment can cause serious environmental damage, including the death of water and plant life, as well as soil deterioration that will affect humans [3]. Lead, for example, is a non-biodegradable metal that is harmful to people and other species and can cause major health problems like anemia [4]. It can enter the food chain, be absorbed, and can accumulate in body tissues [2]. Because of its toxicity, the extent of its contamination in aquatic systems, the potential for major health hazards, and tight requirements, lead must be tested, monitored, and removed from PW before disposal. Pb levels in wastewater and agricultural soils should not exceed 0.01 ppm, according to WHO guidelines [5].

Electrochemical techniques [6], chemical precipitation [7], chemical coagulation [8], membrane filtration [9], ion exchange [10], bioremediation [11], and adsorption [12] have all been used to remove heavy metals in the past. However, the majority of these treatments are inefficient, have limited large-scale operation capability, and are expensive, all of which limit their application. Adsorption is recognized as the most successful physicochemical strategy for heavy metal removal among the other procedures due to its simple operation, cost-effectiveness, and regeneration nature of the adsorbents [13].

The adsorbents that have been investigated for removal of heavy metals include activated carbon [14], cellulose nanofibers [15], biochar [16], zeolites [17], carbon nanotubes [18], agro-industrial waste materials [19], clay minerals [20], and

✉ Bassim H. Hameed
b.hammadi@qu.edu.qa

[1] Department of Chemical Engineering, College of Engineering, Qatar University, P.O. Box 2713, Doha, Qatar

[2] Center for Environmental Studies and Research, Sultan Qaboos University, Al-Khoud 123, Seeb, Oman

[3] Gas Processing Center, College of Engineering, Qatar University, P.O. Box 2713, Doha, Qatar

modified activated carbon [21]. Activated carbon is a desirable adsorbent for heavy metal removal because of its unique features, such as high pore volume and vast surface area [22]. Although a variety of carbon-rich materials can be used to make activated carbon, charcoal is the most common material used in commercial activated carbon manufacturing [23]. Charcoal has a high adsorption efficiency, but it requires a high initial capital cost for large-scale applications. As a result, more focus has been placed on locating inexpensive and unconventional precursors for the manufacture of effective activated carbons, such as agricultural and industrial wastes. The significant increase in the production and distribution of tires over the past two decades initiated the idea of recycling and using the tires in the pyrolysis process to allow for the production of char as a side product, under certain conditions [23]. Char is a very carbonaceous substance that may be utilized as a precursor to create activated carbon for heavy metal adsorption, which is a win–win approach to solve the problem of the waste tire and produce a cost-effective adsorbent.

Although the adsorption tests are considered simple to perform and are carried out in the laboratory, they require a high number of tests and a long time to create the kinetic and isotherms. Using simulation software is beneficial as it saves time and cost, and allows us to find the appropriate operating range by varying different parameters. Software such as Aspen Adsorption® V11 offers the chance of conducting different trials under a wide variety of conditions to determine the optimal conditions. Carrying out simulations at various conditions is safer as parameters such as high concentrations of lead can be studied, whereas in a lab, such experiments are considered to be unsafe. These software programs are particularly useful for small and medium firms that cannot afford more advanced heavy metal wastewater treatment due to running costs [4].

The aforementioned literature review suggests that a new inexpensive and sustainable adsorbent is required to treat industrial PW. There is a crucial need to develop and use simulation protocol to test the removal efficiencies of such adsorbents, and there is a gap in knowledge regarding the feasibility of using software to scale up and optimize the adsorption process. Therefore, the objectives of this work are to simulate a fixed-bed column for the adsorption of lead(II) using two types of activated carbons, tire-derived activated carbon (TAC) and commercial activated carbon (CAC), and to determine their performances by establishing the breakthrough curves using Aspen Adsorption® V11.

2 Methodology

2.1 Physical and chemical properties of lead

The physical and chemical properties of the contaminant, lead, are readily available in the Aspen Properties® version 11 software. The property method used was non-random two-liquid (NRTL). The NRTL model calculates liquid activity coefficients and is recommended for highly non-ideal chemical systems for both vapor–liquid and liquid–liquid equilibrium applications and uses the advanced equation-of-state mixing rules [4].

2.2 Feed and product stream simulation

An input stream, an adsorption tower, or packed-bed column, and a product stream are all part of the process. Figure 1 depicts an activated carbon packed-bed column developed for the simulation. The feed requirements, such as flow rates (9.88×10^{-4} m^3/s, 1.98×10^{-3} m^3/s, 2.96×10^{-3} m^3/s, 3.95×10^{-3} m^3/s, and 4.94×10^{-3} m^3/s) and initial concentration of lead(II) ions (500 mg/L, 1000 mg/L, 2000 mg/L, and 3000 mg/L), were utilized as inputs for the input stream. For the adsorption column setup, the required input values such as the internal diameter of the adsorbent layer and the interparticle voidage were provided as 0.025 m and 0.4, respectively. The feed stream enters at a temperature of 25 °C and a pressure of 3 bar. The product concentration was checked to ensure it was set to zero to establish the breakthrough curves for the adsorption column. The reversible model was selected as the process model type [4]. The feed flow rate was set at the feed block, resulting in a consistent flow rate throughout the adsorption process. This holds true for dilute liquids in which the effect of ions binding to the adsorbent is minimal [4].

2.3 Properties of the adsorbents

Two types of activated carbons were used for the simulation: CAC and TAC [22]. The BET surface area, cumulative

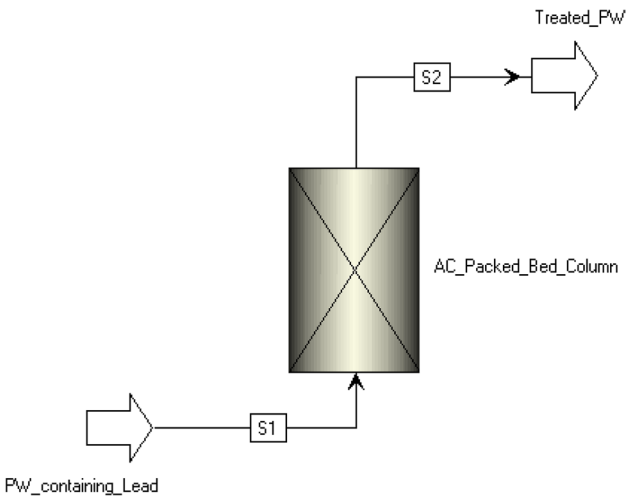

Fig. 1 Simulation flowsheet of liquid-phase adsorption on Aspen Adsorption.® V11

pore volume, pore size, and density for CAC were 1241 m^2/g, 0.445 cm^3/g, 2.781 nm, and 2050 kg/m^3, respectively, whereas for TAC, they were 82 m^2/g, 0.302 cm^3/g, 19.756 nm, and 1940 kg/m^3, respectively [23].

2.4 Packed-bed column specification

The adsorption process was simulated using Aspen Adsorption® V11 with a set of equations that were configured using the tabs, namely the general tab, the material/momentum balance tab, the kinetic model tab, and the isotherm tab. The following theoretical assumptions were made for the bed [4]: (1) discretization model (upwind differencing scheme-first order (UDS 1)), (2) material balance assumption (convection with estimated dispersion), (3) pressure drop assumption (none), (4) velocity assumption (constant), (5) film model assumption (solid), (6) kinetic model assumption (linear lumped resistance), (7) form of mass transfer coefficient (constant), (8) isotherm assumed for layer (Langmuir 1 model), and (9) energy balance assumption (isothermal).

The UDS 1 was chosen as the discretization method under the general tab because it is an excellent all-around performer, non-oscillatory in all possible situations, and unconditionally stable; takes less time to simulate; and has fair accuracy. The UDS 1 is a first-order upwind differencing scheme based on the Taylor expansion of the first order [4].

This equation depicts the first-order convection term:

$$\frac{\partial \Gamma_i}{\partial z} = \frac{\Gamma_i - \Gamma_{i-1}}{\Delta z} \tag{1}$$

whereas the second-order dispersion term is shown using a second-order differencing scheme:

$$\frac{\partial^2 \Gamma_i}{\partial z^2} = \frac{\Gamma_{i+1} - 2\Gamma_i + \Gamma_{i-1}}{\Delta z^2} \tag{2}$$

where Γ is the dependent variable and z is the independent spatial variable.

The number of nodes was kept as the default in the program and was set as 20. The essential assumptions regarding material dispersion in the liquid phase for the ion exchange process are provided in the material/momentum balance tab. Convection with estimated dispersion was used as the material/momentum balance assumption. The dispersion term for the material balance of the bed is included in this assumption. Within the length of the bed, the dispersion coefficient varies. The program, in this situation, is capable of combining all of the resistances to an overall mass transfer single component. The linear lumped resistance model was chosen from the kinetic model tab. The mass transfer driving force for component i is represented as a linear function of the solid phase loading:

$$\frac{\partial w_i}{\partial t} = MTC_{si}\left(w_i' - w_i\right) \tag{3}$$

where w_i represents the equilibrium solid loading for component i and MTC_{si} is a constant provided by the user, or they can vary and, in that case, are either estimated by the software's correlations [24]. Because the mass transfer driving force is represented as a function of the solid-phase concentration, the solid film was chosen under the film model assumption. The Langmuir adsorption isotherm models were obtained from previous experimental studies [23]. The Langmuir model equation [25] is

$$q_e = \frac{q_L K_L C_e}{1 + K_L C_e} \tag{4}$$

where q_L represents the maximum monolayer adsorption capacity (mg/g), q_e is the equilibrium adsorption capacity (mg/g), and K_L (L/mg) is Langmuir constant. The Langmuir model parameters, q_{max} and K_L, for both the adsorbents were obtained as 476.2 mg/g and 0.015 L/mg for TAC and as 42.5 mg/g and 0.008 L/mg for CAC, respectively [23].

2.5 Mass transfer coefficient

The external mass transfer coefficient of particles in a fixed column was calculated using the following equation [26]:

$$Sh = 2 + 1.1 Re^{0.6} Sc^{\frac{1}{3}} \tag{5}$$

where $Sh = K_c D_p / D_{AB}$, $Re = D_p u\rho/\mu$, and $Sc = \mu/\rho D_{AB}$. Substituting these parameters results to

$$\frac{K_c D_p}{D_{AB}} = 2 + 1.1\left(\frac{D_p u \rho}{\mu}\right)^{0.6} \left(\frac{\mu}{\rho D_{AB}}\right)^{\frac{1}{3}} \tag{6}$$

where D_p is the average particle diameter in cm, D_{AB} is the mass diffusivity of solute A in solvent B, u is the fluid velocity in m/s, ρ is the density of the solution, and μ is the solution viscosity [4]. The particle size was 0.02 mm, and the viscosity of the solution was 8.94×10^{-4} kg/ms at 25 °C. The density of the solution was calculated at each concentration of lead ranging from 1000.5 to 1003 kg/m^3.

The total mass diffusivity of the electrolyte Pb $(NO_3)_2$ in water was calculated. The diffusion coefficient obtained was 9.45×10^{-10} m^2/s for $D_{Pb}{}^{2+}$ and 19.02×10^{-10} m^2/s for $D_{NO_3^-}$ D_{NO3} [27]. This resulted in the overall D_{AB} value being 1.4175×10^{-9} m^2/s.

The mass transfer coefficient in the adsorption tower was adjusted to be constant across the bed. However, due to the relationship between fluid velocity and fluid flow rate with the mass transfer coefficient, a change is seen in the mass transfer coefficient when the fluid flow rate is altered [28]. Table 1 provides a list of flow rates as well as the

corresponding mass transfer coefficients that were used for the simulation.

2.6 Process simulation

After completing the bed configuration and identifying all necessary parameters, the system was ready to be simulated. Aspen Adsorption® V11 was used to simulate the adsorption of lead(II) ions in the packed-bed column (Fig. 1). The effect of different parameters such as the initial lead(II) concentration, the bed height, and the flow rate was studied to observe each parameter's influence on the breakthrough time.

The simulation began with the process being initialized and then switched to dynamic mode. The breakthrough curve was generated as time progressed in the dynamic model.

The initial concentration of the contaminant was first changed, keeping a constant flow rate (4.94×10^{-4} m^3/s) and bed height (0.4 m). The initial concentrations of lead(II) ions were 500 mg/L, 1000 mg/L, 2000 mg/L, and 3000 mg/L. The optimum initial concentration of the lead(II) ions was determined by studying the breakthrough curves and choosing the concentration which produced a curve with the longest breakthrough time. Next, the height of the bed was changed to observe its effect on the breakthrough time by changing the height in each trial from 0.20 to 0.60 m, with increments of 0.10 m. The optimum concentration of the contaminant found previously was used and kept constant, along with the flow rate at 4.94×10^{-4} m^3/s.

Table 1 Mass transfer coefficients at different flow rates

Velocity (m/s)	Flow rate (m^3/s)	K_c (1/s)
1	4.94×10^{-4}	0.342
2	9.88×10^{-4}	0.519
4	1.98×10^{-3}	0.786
6	2.96×10^{-3}	1.00
8	3.95×10^{-3}	1.19
10	4.94×10^{-3}	1.36

Lastly, the feed flow rate was changed in each trial to observe its effect on the breakthrough time, keeping the concentration and bed height at their optimum values as obtained in the previous trials. Different velocities for the liquid stream flowing (2 m/s, 4 m/s, 6 m/s, 8 m/s, and 10 m/s) were used. The mass transfer coefficient was then calculated for each flow rate and was used each time the flow rate was changed.

These steps were first carried out for the TAC adsorbent followed by the CAC adsorbent.

The optimum produced breakthrough curves for both the adsorbents were then compared.

3 Results and discussion

The adsorption process was simulated with a total of 28 runs with varying lead(II) ion concentrations, flow rates, and bed heights. This was done using a trial-and-error technique, which demonstrated that the chosen values of the parameters were within the range to produce a successful breakthrough curve. A greater or lower value from the range of values indicated that the adsorption process would no longer be efficient due to the breakthrough curves not being successful.

3.1 Effect of lead(II) initial concentration

By changing the initial concentration of lead(II) from 500 to 3000 mg/L at a constant bed height of 0.4 m and flow rate of 4.94×10^{-4} m^3/s, the effect of the initial concentration on the system was evaluated. Figure 2 depicts the breakthrough curves for both the adsorbents (TAC and CAC) for the column. The initial concentrations used for the lead(II) were 500 mg/L, 1000 mg/L, 2000 mg/L, and 3000 mg/L.

It can be seen from Fig. 2 that the outlet concentration of lead(II) increases as the adsorption process proceeds, ultimately reaching the inlet concentration value. It was observed that the breakthrough curves obtained are steeper at high initial concentrations and the curves lost their steepness at low initial concentrations of 500 mg/L, 1000 mg/L, and 2000 mg/L when considering the curves at a constant

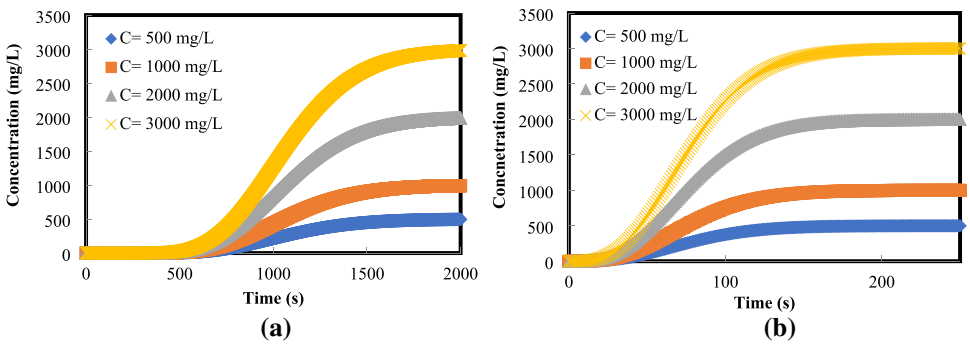

Fig. 2 Comparison of the breakthrough curves at 25 °C and 3 bar with a constant flow rate of 4.94×10^{-4} m^3/s and a bed height of 0.4 m, with varying initial concentrations. **a** TAC. **b** CAC

flow rate and bed height for both adsorbents. The breakthrough times for a concentration of 3000 mg/L were obtained as 639 s and 30 s for TAC and CAC, respectively. At the same concentration, the saturation times obtained for TAC and CAC were 1643 s and 143 s, respectively. Since TAC has a longer breakthrough and saturation time, a larger volume of the solution could be treated and therefore can be considered the better adsorbent. As seen in Table 2, at an initial concentration of 3000 mg/L, the adsorption capacity at $t_{0.5}$ were 681.13 mg/g and 45.82 mg/g for TAC and CAC, respectively. This suggests that for the same length of time, the adsorption capacity ($q_{0.5}$) is higher for TAC and, in this case again, implies that TAC is a better adsorbent due to its higher adsorption capacity. In general, a breakthrough curve reflects how much of an adsorbent bed's capacity was used. The column saturates faster during the adsorption process if the breakthrough curve is steeper, while a less steep breakthrough curve implies low saturation of the column at a low initial metal concentration as there are fewer metal ions present in the solution. This indicates that when the concentration of lead flowing down the column was increased, the pores of the adsorbent will be saturated much quicker and produce a much steeper curve. Increasing the initial concentrations of heavy metal ions increases the driving force at the solid–liquid interface, resulting in increased adsorption capacity until the adsorption sites were saturated. Thus, a shorter breakthrough time is observed for the steeper curves. With a lower initial concentration, a breakthrough curve with a longer breakthrough time was produced, suggesting that a larger volume of solution could be treated. This is because a lower concentration gradient causes a slower transport due to a decrease in diffusion coefficient or mass transfer coefficient [29]. Therefore, the optimum lead(II) initial concentration was 500 mg/L.

Studies carried out previously depict a similar trend of increasing the contaminants' initial concentration on the breakthrough time [30]. It was determined that the adsorption capacity of heavy metal ions increased, and the removal efficiency decreased with the increasing initial concentrations of heavy metal ions.

When plotting C/C_0 vs. time, the simulation data overlaps. This means there is no correlation between initial lead(II) concentration and breakthrough or saturation time. However, according to Alhamed [31], this is not the true

Table 2 Column adsorption capacity at different initial lead(II) concentrations, bed heights, and flow rates for both adsorbents (TAC and CAC) at $t_{0.5}$

Adsorbent	Initial lead(II) concentration (mg/L)	Bed height (m)	Flow rate (m^3/s)	Mass (g)	$t_{0.5}$ (s)	Adsorption capacity, $q_{0.5}$ (mg/g)
TAC	500	0.4	4.94E − 04	2.30	1055	113.52
	1000	0.4	4.94E − 04	2.30	1054	226.83
	2000	0.4	4.94E − 04	2.30	1055	454.09
	3000	0.4	4.94E − 04	2.30	1055	681.13
	500	0.2	4.94E − 04	1.15	517	111.26
	500	0.3	4.94E − 04	1.73	786	112.77
	500	0.5	4.94E − 04	2.88	1324	113.97
	500	0.6	4.94E − 04	3.45	1593	114.27
	500	0.6	9.88E − 04	3.45	798	114.26
	500	0.6	1.98E − 03	3.45	399	114.49
	500	0.6	2.96E − 03	3.45	268	114.96
	500	0.6	3.95E − 03	3.45	201	115.06
	500	0.6	4.94E − 03	3.45	161	115.26
CAC	500	0.4	4.94E − 04	2.43	75	7.64
	1000	0.4	4.94E − 04	2.43	75	15.27
	2000	0.4	4.94E − 04	2.43	75	30.55
	3000	0.4	4.94E − 04	2.43	75	45.82
	500	0.2	4.94E − 04	1.22	37	7.54
	500	0.3	4.94E − 04	1.82	56	7.60
	500	0.5	4.94E − 04	3.04	94	7.66
	500	0.6	4.94E − 04	3.65	113	7.67
	500	0.6	9.88E − 04	3.65	57	7.72
	500	0.6	1.98E − 03	3.65	29	7.87
	500	0.6	2.96E − 03	3.65	20	8.12
	500	0.6	3.95E − 03	3.65	15	8.13
	500	0.6	4.94E − 03	3.65	12	8.13

phenomenon. Another possibility is that the kinetic model's assumption of linear lumped resistance may not properly reflect the entire mechanism of phenol adsorption onto activated carbon particles.

3.2 Effect of bed height

Using the best initial lead(II) concentration of 500 mg/L obtained from the previous simulations, the bed height was varied from 0.2 to 0.6 m, in increments of 0.1 m, at a constant flow rate of 4.94×10^{-4} m^3/s. Figure 3 shows the breakthrough curves obtained for the column at different bed heights.

As the bed height was increased, the breakthrough curve became less steep. This can be seen as the breakthrough time was obtained as 237 s for TAC and 11 s for CAC at a bed height of 0.2 m. On the other hand, at the bed height of 0.6 m, a breakthrough time of 994 s and 52 s was obtained for TAC and CAC, respectively. With a higher bed height, the breakthrough time increased, resulting in a greater lead(II) removal efficiency because there is good contact time between the metal ions and the adsorbent. A greater bed height provides more binding sites for the adsorption process and a larger surface area, resulting in a longer breakthrough time and, as a result, a higher removal rate of lead(II). A lower bed height indicates that the bed has a reduced ability to adsorb metal ions from the solution due to its smaller surface area, resulting in the binding sites being occupied more quickly and therefore having a shorter breakthrough time. In addition, at lower bed heights, axial dispersion is the primary mass transfer process, reducing metal ion diffusion [32]. Using Table 2, it can be seen that at a bed height of 0.6 m, the adsorption capacity at $t_{0.5}$ was 114.27 mg/g and 7.67 mg/g for TAC and CAC, respectively. Since a longer breakthrough and saturation time is obtained for the adsorbent TAC which, in turn, results in having a higher adsorption capacity ($q_{0.5}$), this suggests that TAC is a better adsorbent due to having a higher adsorption capacity at the same conditions compared to CAC. The best bed height was, therefore, determined to be 0.6 m, which resulted in a breakthrough curve with the longest breakthrough time and the least steep curve.

A similar trend was obtained by Firdaus et al. [33] when studying the effect of changing the bed height on the adsorption process of copper(II) from wastewater using corncob-based activated carbon (CCAC) at room temperature. It was seen that increasing the bed height enhanced the breakthrough and exhaustion time. This is because as the bed height was increased, the total surface area of the adsorbent increased as well. The functional groups present such as carboxyl and hydroxyl groups on the surface of the adsorbent CCAC also show good coordination with heavy metals which is enhanced with a larger surface area. As a result, an increase in the adsorption binding sites can be seen with an increase in bed height, causing a better metal absorption capacity and a longer breakthrough time.

3.3 Effect of feed flow rate

The used flow rates (9.88×10^{-4} to 4.94×10^{-3} m^3/s) and the breakthrough curves for a column system with a bed height of 0.6 m and metal ion initial concentration of 500 mg/L are depicted in Fig. 4. It can be observed from the breakthrough curves that increasing the flow rate resulted in a steeper curve. A breakthrough time of 89 s and 3.5 s was obtained for TAC and CAC, respectively, at a flow rate of 4.94×10^{-3} m^3/s. Similarly, the saturation time obtained for TAC and CAC at the same flow rate was 260 s and 30 s, respectively.

This implies that greater fluid movement resulted in quicker saturation of the adsorbent pores, as the velocity of the contaminant entering the pores of the adsorbent also increased. At higher flow rates, the contact time between the adsorbent and the lead ions is reduced, resulting in a shorter contract period. As a result, a thin film forms around the adsorbent which causes the rate of mass transfer to increase, and the quantity of lead adsorbed onto the bed to increase as well, resulting in faster saturation at higher flow rates [34]. It can be seen in Table 2 that at a flow rate of 4.94×10^{-3} m^3/s, the adsorption capacity at $t_{0.5}$ was 115.26 mg/g and 8.13 mg/g for TAC and CAC, respectively. A longer breakthrough and saturation time is obtained for the adsorbent TAC which, in

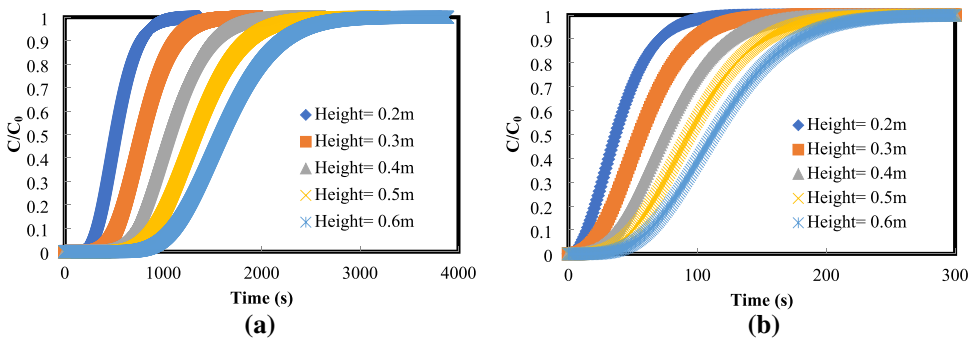

Fig. 3 Comparison of the breakthrough curves at 25 °C and 3 bar with a constant flow rate of 4.94×10^{-4} m^3/s and lead(II) initial concentration of 500 mg/L, at different bed heights. **a** TAC. **b** CAC

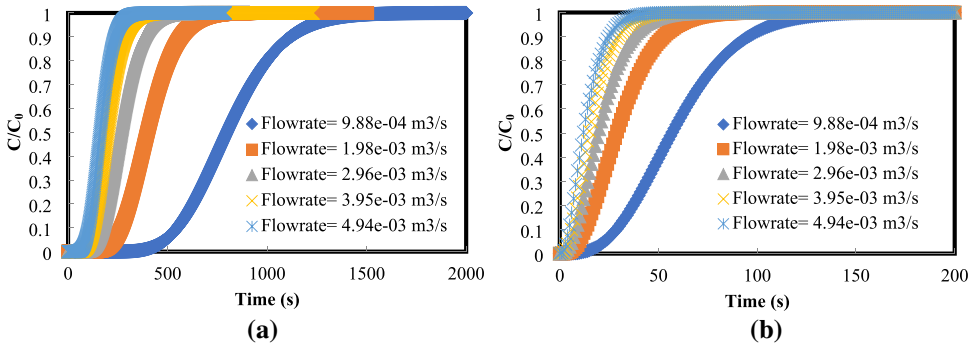

Fig. 4 Comparison of the breakthrough curves at 25 °C and 3 bar with a constant initial concentration of 500 mg/L and a bed height of 0.6 m, with varying flow rates. **a** TAC. **b** CAC

turn, has a higher adsorption capacity, suggesting that TAC is a better adsorbent due to its higher adsorption capacity under the same conditions compared to CAC.

A breakthrough time of 488 s was obtained for TAC and 23 s for CAC at a flow rate of 9.88×10^{-4} m^3/s. The external film mass resistance at the adsorbent's surface rose as the flow rate decreased, as did the residence time. As a result, the time required for saturation increased, suggesting good absorption and a longer time for a breakthrough. Therefore, the optimum flow rate for the removal of lead from produced water was 9.88×10^{-4} m^3/s.

Experiments carried out by Kavand et al. [35] explain a similar trend to what was obtained through our simulations. The results from their studies show that as the flow rate increases from 1 to 5 ml/min, the time to reach the breakthrough point decreases from 450 to 100 min. This is because when the flow rate increases, the residence time of the solute in the bed reduces, leaving insufficient time for adsorption equilibrium to be established, resulting in decreased bed utilization and the adsorbate solution leaving the column before equilibrium.

3.4 Comparison between TAC and CAC performances

The results of the simulations revealed that the most optimum conditions were found to be the initial lead concentration of 500 mg/L with a bed height of 0.6 m and a flow rate of 9.88×10^{-4} m^3/s. This was the case for both the adsorbents, TAC and CAC. At these optimum conditions, the breakthrough curves of both the adsorbents were plotted to compare their breakthrough times as shown in Fig. 5.

It can be seen that the breakthrough time obtained for CAC was 7 s, whereas for TAC, it was 391 s, depicting that it takes much longer for TAC to get saturated with lead. This suggests that TAC is a better adsorbent at these optimum conditions to adsorb lead from PW for the longest period. The adsorption capacities calculated at the varying conditions for both the adsorbents in Table 2 also suggest that TAC is a better adsorbent due to its higher adsorption capacities. The BET surface area suggests that CAC has a

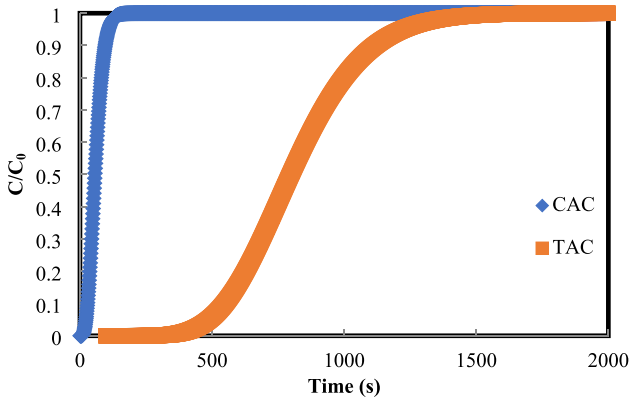

Fig. 5 Comparison between TAC and CAC breakthrough curves at optimum conditions

higher surface area to allow more of the lead to be adsorbed from the PW; however, this is not seen from the results of the simulation. From the FT-IR results obtained from previous studies, it is determined that both CAC and TAC show peaks forming at wavelengths corresponding to carboxylic, hydroxyl, and phenolic groups. Higher intensities of these groups are seen for TAC, suggesting an increase in the coordination of TAC with heavy metals. Another reason for TAC to be the better adsorbent may be due to its better accessibility because of its higher pore size. As a result, TAC has a higher affinity towards the lead(II) than CAC.

These generated breakthrough curves can offer a basic overview of which adsorbent is preferable. However, in order to determine the numerical values for adsorption capacities, computations are required to validate the accuracy of the assumptions made. The mass of the adsorbent is estimated by determining the volume of the packed-bed column and then using 60% of that value as the volume that is packed with the adsorbent to calculate the adsorption capacity.

The amount of lead(II) adsorbed at $q_{0.5}$ (mg/g) is calculated using the following equation [36]:

$$q_{0.5} = \frac{t_{0.5} \times F \times C_0}{m_{\text{adsorbent}}} \tag{7}$$

where F (m^3/s) is the volumetric flow rate of lead(II), m (g) is the mass of adsorbent in the adsorption column, C_0 is the inlet concentration of lead(II), and $t_{0.5}$ is half of the total adsorption time.

Due to the values of the adsorption capacity at breakthrough and saturation time, a method developed by Chowdhury et al. [29] was adopted to compute the adsorption capacities at $t_{0.5}$.

Using the results generated above, further dynamic adsorption parameters such as length of mass transfer zone (MTZ), empty bed contact time (EBCT), degree of sorbent used (DoSU), and sorbent usage rate (SUR) were obtained from the breakthrough data through the equations used by Nwabanne et al. [37]. The param eters obtained are listed in Table 3. It can be seen from Table 3 that as the concentration increases, the DoSU increases. The reason is connected to a higher concentration of the lead(II) present in the wastewater which, in turn, allows more of the pollutant to be adsorbed. In terms of the bed height, it can be seen that as the bed height increases, both MTZ and DoSU increase as well. A greater bed height indicates a larger amount of adsorbent and mass transfer zone, which increases the amount of sorbent used and the volume of effluent treated. With the increase in flow rate, the MTZ value decreases for both the adsorbents. An increased flow rate indicates a reduction in the residence time of lead, and because lead did not have enough time to diffuse into the active pores of the adsorbent, it leaves the column unadsorbed and therefore has a smaller mass transfer zone.

4 Conclusion

Simulations were carried out using Aspen Adsorption® V11 to imitate a fixed packed-bed column, and the breakthrough curves were analyzed for different parameters such as initial lead(II) concentration, bed height, and produced water flow rate. A prolonged breakthrough time indicated a high adsorption capacity. Increasing the initial lead concentration and flow rate both resulted in a quicker breakthrough time since the adsorbent saturated faster and there was a decrease in contact time between the contaminant and the adsorbent. Increased bed height had the opposite effect, resulting in more binding sites for adsorption and hence a slower breakthrough time. With a flow rate of 9.88×10^{-4} m^3/s, an initial contaminant concentration of 500 mg/L, and a bed height of 0.6 m, the slowest breakthrough time was 488 s for TAC and 23 s for CAC. The results indicated that the performance of the TAC was better in adsorbing lead(II) ions compared to the commercial activated carbon. It may be concluded that tire-derived activated carbon has a significant potential as a cost-effective alternative adsorbent material for heavy metal removal, thereby reducing waste tire disposal problems.

Table 3 Breakthrough parameters for the adsorption of lead(II) onto TAC and CAC

Adsorbent	Column adsorption parameters	Process variables														
		Concentration (mg/L)				Bed height (m)						Flow rate (m^3/s)				
		500	1000	2000	3000	0.2	0.3	0.4	0.5	0.6	4.94E−04	9.88E−04	1.98E−03	2.96E−03	3.95E−03	4.94E−03
TAC	DoSU	0.238	0.476	0.954	1.430	0.153	0.229	0.238	0.239	0.240	0.240	0.240	0.240	0.241	0.242	0.242
	SUR (g/L)	0.004	0.004	0.004	0.004	0.005	0.004	0.004	0.004	0.004	0.004	0.004	0.004	0.004	0.004	0.004
	MTZ (m)	0.305	0.209	0.019	0.172	0.153	0.229	0.305	0.380	0.456	0.456	0.456	0.456	0.455	0.455	0.455
	EBCT (min)	2.400	2.400	2.400	2.400	1.200	1.805	2.400	3.005	3.600	3.600	1.800	0.898	0.601	0.450	0.360
CAC	DoSU	0.180	0.359	0.719	1.078	0.177	0.179	0.180	0.180	0.180	0.180	0.182	0.185	0.191	0.191	0.191
	SUR (g/L)	0.066	0.066	0.066	0.066	0.067	0.066	0.066	0.065	0.065	0.065	0.065	0.064	0.062	0.062	0.062
	MTZ (m)	0.328	0.256	0.112	0.031	0.165	0.246	0.328	0.410	0.492	0.492	0.491	0.489	0.485	0.485	0.485
	EBCT (min)	0.341	2.400	2.400	2.400	2.400	1.205	0.341	1.797	3.002	3.002	3.604	1.802	0.899	0.602	0.451

Acknowledgements The findings achieved herein are solely the responsibility of the authors.

Author contribution Conceptualization: Bassim H. Hameed and Muhammad Usman; investigation: Areeba Hameed; data curation: Areeba Hameed; writing and preparation of the original draft: Areeba Hameed; formal analysis: Areeba Hameed; validation: Bassim Hamid Hameed, Muhammad Usman, and Fares A. Almomani; writing including reviewing and editing: Bassim Hamid Hameed, Fares A. Almomani, Muhammad Usman, Muneer M. Ba-Abbad, and Majeda Khraisheh. All authors read and approved the final manuscript.

Funding Open Access funding provided by the Qatar National Library. This publication was jointly supported by the Qatar University and Sultan Qaboos University, Oman, under the international research collaboration grant (IRCC-2021–014; CL/SQU-QU/CESR/21/01).

Data availability All data generated or analyzed during this study are included in this manuscript.

Declarations

Conflict of interest The authors declare no competing interests.

Open Access This article is licensed under a Creative Commons Attribution 4.0 International License, which permits use, sharing, adaptation, distribution and reproduction in any medium or format, as long as you give appropriate credit to the original author(s) and the source, provide a link to the Creative Commons licence, and indicate if changes were made. The images or other third party material in this article are included in the article's Creative Commons licence, unless indicated otherwise in a credit line to the material. If material is not included in the article's Creative Commons licence and your intended use is not permitted by statutory regulation or exceeds the permitted use, you will need to obtain permission directly from the copyright holder. To view a copy of this licence, visit http://creativecommons.org/licenses/by/4.0/.

References

1. Yousef R, Qiblawey H, El-Naas MH (2020) Adsorption as a process for produced water treatment: a review. Processes 8:1–22
2. Arbabi M, Hemati S, Amiri M (2015) Removal of lead ions from industrial wastewater: a review of removal methods. Int J Epidemiol Res 2:105–109
3. Qasem NAA, Mohammed RH, Lawal DU (2021) Removal of heavy metal ions from wastewater: a comprehensive and critical review. npj Clean Water 4:36. https://doi.org/10.1038/s41545-021-00127-0
4. Nieva AD, Garcia RC, Ped RMR (2019) Simulated biosorption of Cr6+ using peels of Litchi chinensis Sonn by Aspen Adsorption® V84. Int J Environ Sci Develop 10:331–337. https://doi.org/10.18178/ijesd.2019.10.10.1195
5. Kinuthia GK, Ngure V, Beti D et al (2020) Levels of heavy metals in wastewater and soil samples from open drainage channels in Nairobi, Kenya: community health implication. Scientific Reports 10. https://doi.org/10.1038/s41598-020-65359-5
6. Mohanakrishna G, Al-Raoush RI, Abu-Reesh IM (2021) Integrating electrochemical and bioelectrochemical systems for energetically sustainable treatment of produced water. Fuel 285. https://doi.org/10.1016/j.fuel.2020.119104
7. Barakat MA (2011) New trends in removing heavy metals from industrial wastewater. Arab J Chem 4:361–377
8. Rodriguez AZ, Wang H, Hu L et al (2020) Treatment of produced water in the Permian Basin for hydraulic fracturing: comparison of different coagulation processes and innovative filter media. Water (Switzerland) 12. https://doi.org/10.3390/w12030770
9. Kárászová M, Bourassi M, Gaálová J (2020) Membrane removal of emerging contaminants from water: which kind of membranes should we use? Membranes (Basel) 10:1–23. https://doi.org/10.3390/membranes10110305
10. Vaudevire E, Radmanesh F, Kolkman A et al (2019) Fate and removal of trace pollutants from an anion exchange spent brine during the recovery process of natural organic matter and salts. Water Res 154:34–44. https://doi.org/10.1016/j.watres.2019.01.042
11. Epa U, of Solid Waste O, Response E (2013) Introduction to in situ bioremediation of groundwater
12. Khader EH, Mohammed TJ, Mirghaffari N et al (2021) Removal of organic pollutants from produced water by batch adsorption treatment. Clean Technol Environ Policy. https://doi.org/10.1007/s10098-021-02159-z
13. Vo TS, Hossain MM, Jeong HM et al (2020) Heavy metal removal applications using adsorptive membranes. Nano Converg 7:36. https://doi.org/10.1186/s40580-020-00245-4
14. Filho AV, Kulman RX, Tholozan LV et al (2020) Preparation and characterization of activated carbon obtained from water treatment plant sludge for removal of cationic dye from wastewater. Processes 8:1–13. https://doi.org/10.3390/pr8121549
15. Amin NAAM, Mokhter MA, Salamun N, Mahmood WMAW (2021) Phosphate adsorption from aqueous solution using electrospun cellulose acetate nanofiber membrane modified with graphene oxide/sodium dodecyl sulphate. Membranes (Basel) 11. https://doi.org/10.3390/membranes11070546
16. Srivatsav P, Bhargav BS, Shanmugasundaram V et al (2020) Biochar as an eco-friendly and economical adsorbent for the removal of colorants (dyes) from aqueous environment: a review. Water (Switzerland) 12
17. Tasić ŽZ, Bogdanović GD, Antonijević MM (2019) Application of natural zeolite in wastewater treatment: a review. J Min Metallurgy A: Min 55:67–79. https://doi.org/10.5937/jmma1901067t
18. Arora B, Attri P (2020) Carbon Nanotubes (CNTs): A Potential Nanomaterial for Water Purification. J Comp Sci 4(3):135
19. Akratos CS, Tekerlekopoulou AG, Vayenas DV (2021) Agro-Industrial Wastewater Treatment with Decentralized Biological Treatment Methods. Water 13(7):953
20. Jellali S, Khiari B, Usman M, Hamdi H, Charabi Y, Jeguirim M (2021) Sludge-derived biochars: A review on the influence of synthesis conditions on pollutants removal efficiency from wastewaters. Renew Sust Energ Rev144:111068. https://doi.org/10.1016/j.rser.2021.111068
21. Jiang C, Cui S, Han Q et al (2019) Study on application of activated carbon in water treatment. In: IOP Conference Series. Earth Environ Sci 237:022049
22. Liu Y, Xu X, Qu B et al (2021) Study on adsorption properties of modified corn cob activated carbon for mercury ion. Energies (Basel) 14. https://doi.org/10.3390/en14154483
23. Shahrokhi-Shahraki R, Benally C, El-Din MG, Park J (2021) High efficiency removal of heavy metals using tire-derived activated carbon vs commercial activated carbon: insights into the adsorption mechanisms. Chemosphere 264. https://doi.org/10.1016/j.chemosphere.2020.128455
24. Welty JR, Wicks CE, Wilson RE (1976) Fundamentals of momentum, heat, and mass transfer. New York: Wiley
25. Chemical Engineering Software: Model mass and energy balances. COMSOL. (1998) Retrieved March 24, 2022. from https://www.comsol.com/chemical-reaction-engineering-module

26. Patel MS, Talu O (2017, September 28) Evaluation of mass transfer rate in column of small lilsx particles. Engaged Scholarship. https://engagedscholarship.csuohio.edu/etdarchive/996/
27. Buffle J, Zhang Z, Startchev K (2007) Metal flux and dynamic speciation at (bio)interfaces. Part I: Critical evaluation and compilation of physicochemical parameters for complexes with simple ligands and fulvic/humic substances. Environ Sci Technol 41(22):7609–7620. https://doi.org/10.1021/es070702p
28. Stoodley P, Yang S, Lappin-Scott H, Lewandowski Z (1997) Relationship between mass transfer coefficient and liquid flow velocity in heterogenous biofilms using microelectrodes and confocal microscopy. Biotechnol Bioeng 56:681–688. https://doi.org/10.1002/(SICI)1097-0290(19971220)56:6%3c681::AID-BIT11%3e3.0.CO;2-B
29. Chowdhury ZZ, Zain SM, Rashid AK et al (2013) Breakthrough curve analysis for column dynamics sorption of Mn(II) ions from wastewater by using *Mangostana garcinia* peel-based granular-activated carbon. J Chem. https://doi.org/10.1155/2013/959761
30. Ouyang D, Zhuo Y, Hu L et al (2019) Research on the adsorption behavior of heavy metal ions by porous material prepared with silicate tailings. Minerals 9. https://doi.org/10.3390/min9050291
31. Alhamed Y (2009) Adsorption kinetics and performance of packed bed adsorber for phenol removal using activated carbon from dates' stones. J Hazard Mater 170:763–770. https://doi.org/10.1016/j.jhazmat.2009.05.002
32. Patel H (2020) Batch and continuous fixed bed adsorption of heavy metals removal using activated charcoal from neem (Azadirachta indica) leaf powder. Sci Rep 10. https://doi.org/10.1038/s41598-020-72583-6
33. Yusop, Mohamad & Azmier, Mohd & Yahaya, Nasehir & Karim, Jamilah & Bin Mohamed Yusoff, Muhammad & Hashim, Noor Haza Fazlin & Abdullah, Nor Salmi. (2020). Effect Bed Height on Adsorption of Cu(II) by Using Corncob Based Activated Carbon.https://doi.org/10.2991/aer.k.201229.023
34. Samarghandi MR, Hadi M, McKay G (2014) Breakthrough Curve Analysis for Fixed-Bed Adsorption of Azo Dyes Using Novel Pine Cone—Derived Active Carbon. Adsorption Sci Technol 32(10):791–806. https://doi.org/10.1260/0263-6174.32.10.791
35. Kavand M, Fakoor E, Mahzoon S, Soleimani M (2018) An improved film–pore–surface diffusion model in the fixed-bed column adsorption for heavy metal ions: single and multi-component systems. Process Saf Environ Prot 113:330–342. https://doi.org/10.1016/j.psep.2017.11.009
36. Chowdhury Z, Hamid S, Zain S (2014) Evaluating Design Parameters for Breakthrough Curve Analysis and Kinetics of Fixed Bed Columns for Cu(II) Cations Using Lignocellulosic Wastes. BioResources 10(1):732–749
37. Nwabanne JT, Iheanacho OC, Obi CC, Onu CE (2022) Linear and nonlinear kinetics analysis and adsorption characteristics of packed bed column for phenol removal using rice husk-activated carbon. Appl Water Sci 12:91. https://doi.org/10.1007/s13201-022-01635-1

Publisher's note Springer Nature remains neutral with regard to jurisdictional claims in published maps and institutional affiliations.